DYNAMICAL NUMERICAL PREDICTION OF LARGE-SCALE THERMAL ANOMALIES IN THE NORTH PACIFIC OCEAN

Wayne Stuart Shiver

NAVAL POSTGRADUATE SCHOOL
Monterey, California

THESIS

DYNAMICAL NUMERICAL PREDICTION OF
LARGE-SCALE THERMAL ANOMALIES
IN THE NORTH PACIFIC OCEAN

by

Wayne Stuart Shiver

December 1977

Thesis Advisor: R. L. Haney

SECURITY CLASSIFICATION OF THIS PAGE (When Data Entered)

REPORT DOCUMENTATION PAGE

READ INSTRUCTIONS BEFORE COMPLETING FORM

1. REPORT NUMBER	2. GOVT ACCESSION NO. / 3. RECIPIENT'S CATALOG NUMBER
4. TITLE (and Subtitle): Dynamical Numerical Prediction of Large-Scale Thermal Anomalies in the North Pacific Ocean	5. TYPE OF REPORT & PERIOD COVERED: Master's Thesis; December 1977
	6. PERFORMING ORG. REPORT NUMBER
7. AUTHOR(s): Wayne Stuart Shiver	8. CONTRACT OR GRANT NUMBER(s)
9. PERFORMING ORGANIZATION NAME AND ADDRESS: Naval Postgraduate School, Monterey, California 93940	10. PROGRAM ELEMENT, PROJECT, TASK AREA & WORK UNIT NUMBERS
11. CONTROLLING OFFICE NAME AND ADDRESS: Naval Postgraduate School, Monterey, California 93940	12. REPORT DATE: December 1977
	13. NUMBER OF PAGES: 47
14. MONITORING AGENCY NAME & ADDRESS (if different from Controlling Office): Naval Postgraduate School, Monterey, California 93940	15. SECURITY CLASS. (of this report): Unclassified
	15a. DECLASSIFICATION/DOWNGRADING SCHEDULE

16. DISTRIBUTION STATEMENT (of this Report)

Approved for public release; distribution unlimited.

17. DISTRIBUTION STATEMENT (of the abstract entered in Block 20, if different from Report)

18. SUPPLEMENTARY NOTES

19. KEY WORDS (Continue on reverse side if necessary and identify by block number)

20. ABSTRACT (Continue on reverse side if necessary and identify by block number)

A ten-level primitive equation ocean circulation model is used to investigate the formation and evolution of large-scale thermal anomalies observed in the central North Pacific Ocean during the fall and winter of 1976. Several initial value model integrations of 4 months duration are carried out in order to help explain the observed anomaly development. Initial and verifying ocean data down to 400 m

DD FORM 1 JAN 73 1473 EDITION OF 1 NOV 65 IS OBSOLETE
S/N 0102-014-6601 |
(Page 1)

SECURITY CLASSIFICATION OF THIS PAGE (When Data Entered)

depth are obtained from the NORPAX ships of opportunity program. Anomalous atmospheric wind forcing is obtained from Namias' monthly mean sea-level pressure anomalies, while climatological heat fluxes are used.

The skill with which the model simulates the observed anomaly evolution in the different experiments is estimated synoptically and measured statistically by calculating root mean square (RMS) temperature errors and S1 skill scores. Analysis indicates that anomalous atmospheric wind forcing improves the model predictions in the upper levels. For this particular winter case using climatological heating, however, knowledge of the initial anomalous temperature conditions does not improve the model results. The model skill at upper levels exceeds both persistence and climatology (forecast of zero anomaly) while at the lower levels it is comparable to persistence but not as good as climatology.

Approved for public release; distribution unlimited.

Dynamical Numerical Prediction of Large-Scale Thermal Anomalies in the North Pacific Ocean

by

Wayne Stuart Shiver
Lieutenant, United States Navy
B.S., University of North Carolina, 1972

Submitted in partial fulfillment of the
requirements for the degree of

MASTER OF SCIENCE IN METEOROLOGY AND OCEANOGRAPHY

from the

NAVAL POSTGRADUATE SCHOOL
December 1977

ABSTRACT

A ten-level primitive equation ocean circulation model is used to investigate the formation and evolution of large-scale thermal anomalies observed in the central North Pacific Ocean during the fall and winter of 1976. Several initial value model integrations of 4 months duration are carried out in order to help explain the observed anomaly development. Initial and verifying ocean data down to 400 m depth are obtained from the NORPAX ships of opportunity program. Anomalous atmospheric wind forcing is obtained from Namias' monthly mean sea-level pressure anomalies, while climatological heat fluxes are used.

The skill with which the model simulates the observed anomaly evolution in the different experiments is estimated synoptically and measured statistically by calculating root mean square (RMS) temperature errors and S1 skill scores. Analysis indicates that anomalous atmospheric wind forcing improves the model predictions in the upper levels. For this particular winter case using climatological heating, however, knowledge of the initial anomalous temperature conditions does not improve the model results. The model skill at upper levels exceeds both persistence and climatology (forecast of zero anomaly) while at the lower levels it is comparable to persistence but not as good as climatology.

TABLE OF CONTENTS

LIST OF TABLES

LIST OF FIGURES

ACKNOWLEDGMENTS

The author wishes to express his appreciation to Dr. Robert L. Haney for his guidance, kind understanding and counsel in the preparation of this thesis and to Dr. R. J. Renard for reading the thesis and making many valuable comments.

Special thanks are extended to Drs. R. L. Bernstein and W. B. White of Scripps Institution for their graciously allowing the use of the TRANSPAC XBT data. Appreciation also goes to Dr. J. Namias of Scripps for the use of his sea level pressure anomaly data for September 1976 to January 1977.

I. INTRODUCTION

Early investigations by Namias and others indicated that the winds are an important source of kinetic energy for the oceanic circulation. But just as the mean atmospheric circulation helps drive the mean large scale ocean circulation, anomalous atmospheric forcing can be assumed to drive anomalous currents in the ocean (Malkus, 1962). This premise was, in part, the motivating force for the present model study. The effects of anomalous atmospheric forcing on the oceans have been a matter of intuitive guessing for years, but few studies have attempted to assess in more than a descriptive or qualitative manner the nature or magnitude of these effects. A notable exception is the recent work of Davis (1976, 1977).

One of the most important manifestations of the effects of anomalous atmospheric forcing on the oceans is the deviation of the ocean thermal structure from the long term climatological norm. The space and time scales of these deviations or anomalies are known in a very general sense, but the exact generating mechanism or mechanisms remain unclear at present. It is the intent of this investigation, within the larger context of the Anomaly Dynamics Study (ADS), to "Describe and understand the mechanisms responsible for large scale climatological anomalies and related changes in the thermal structure and the general circulation of the

upper layers of the ocean in order to predict their formation and evolution." (Kirwan, 1976) The contribution of anomalous atmospheric wind forcing as a generating mechanism for changes in the thermal structure of the ocean will be emphasized.

Previous model investigations of the dynamics of large scale temperature anomaly formation in the ocean have been limited by the lack of verifying data, at the surface and at depth, over sufficiently large areas. In cases where anomalous atmospheric forcing for a certain period of time was added to climatological wind forcing (Namias, 1965; Arthur, 1966; Jacob, 1967), model results show an important influence on the ocean by the anomalous forcing.

In the present study, an ocean circulation model is used to make a number of initial value predictions of the evolution of large scale ocean anomalies. The different model predictions are designed to examine the effect on the prediction of including or excluding certain physical processes in the model. The study is unique in that a carefully collected and analyzed set of ocean temperature data are used.

It must be emphasized at this point that this study is not meant to be a test of the predictive capability of the model itself. First, a very important part of the atmospheric forcing fields, namely anomalous heat flux that is required for the testing of the prediction capabilities of any ocean model is not available on the time or space scales

required. Consequently, only anomalous winds are used in the present studies. Second, ocean modeling itself is still relatively unsophisticated and certainly untested in modeling large scale thermal anomalies observed in the oceans even if all the atmospheric forcing were known. In addition, this study will serve as an initial investigation into the adequacy of currently available temperature data in describing the true thermal condition of the Central Pacific. With the current oceanic and atmospheric data available and with the current state of the science of ocean modeling, all that can be tested are a number of hypotheses regarding the relative importance of various dynamic forces that act to drive the oceans. Any conclusions resulting from this study then are subject to re-evaluation as ocean modeling and monitoring capabilities improve. The 1976-77 fall-winter period was selected for this study because of the large amplitude anomalies in the atmosphere and ocean that existed in the North Pacific at that time.

II. DATA PROCESSING

The modeling experiments described below made use of anomalous atmospheric winds and oceanic temperatures. The first step in preparing the atmospheric data for input into the ocean model was calculation of sea-level pressure anomalies or departures from normal for all of 1976 and January and February of 1977. All the atmospheric data were generously made available to us by Dr. J. Namias of Scripps. Long term (20 year) mean values of sea level pressure for each of these months, as determined by Namias, were subtracted from monthly means in order to obtain the sea level pressure departures from norm. Analysis of these anomaly fields indicated the period from September 1976 until January 1977 exhibited sufficiently large anomalous sea level pressures to be suitable for our investigation.

In order then to input Namias' anomalous pressure data into the model, it was necessary to extrapolate and then interpolate the values from Namias' 5° latitude by 5° longitude (9x19) fields encompassing 20°N to 60°N and 145°E to 125°W to the 33x33 fields extending from the equator to 65°N and 145°E to 125°W required by the model (see figure 1). The extrapolation of the anomalous pressure data toward the northern boundary assumed a slope that decreased by 50 percent at each grid point. Extrapolation towards the equator was such that anomalous u and v components of the wind field,

calculated from the anomalous pressures, go to zero at the equator. Once the extrapolation was completed, data north of 50°N was smoothed several times in the east-west direction in order to remove any small scale features introduced by the extrapolation. This procedure was carried out for the months of September 1976 through January 1977.

With the 33x33 field of sea level pressure anomalies computed, the corresponding anomalous geostrophic u and v components of the wind were calculated. These anomalous geostrophic wind fields were the only anomalous atmospheric conditions used in the ocean model. These fields (figure 2) are described in the Results section below.

The next step in data preparation for input into the model was to compute the temperature anomalies that would serve as initial and verifying conditions for the model. All temperature data was provided by TRANSPAC, the ships of opportunity cooperative research effort. The TRANSPAC expendable bathythermograph (XBT) field program is a part of the North Pacific Experiment (NORPAX) which is charged with investigating how oceanic variability influences the weather and climate, and in turn how the weather and climate variability influence the oceanic circulations. Prior to TRANSPAC, data on the thermal structure of the ocean was inadequate, thus leading to the inception of the TRANSPAC XBT field program to provide the subsurface temperature data necessary for NORPAX. The observational phase of the program began in January 1975 utilizing ships of opportunity (i.e. merchant

ships voluntarily providing a no-cost observation platform) that routinely traverse the sea lanes between the United States and Japan. The temperature anomaly data provided through TRANSPAC was obtained by subtracting climatology means from the monthly mean observed temperatures. Anomalous temperatures were provided at ten levels including 0,30, 60, 90, 120, 150, 200, 250, 300 and 400 meters. For initializing temperature fields in the model, the anomalous temperature field for September 1976 was added to the model generated climatology for September. Calculation of verification statistics entailed use of anomalous temperature fields for October through December of 1976 and January 1977. Again, the TRANSPAC anomaly data had to be processed for use in the model because the domain and standard levels of the TRANSPAC data did not coincide with the domain and standard levels of the model. It was decided, in order to avoid major changes to the model, to extrapolate from the 2° latitude by 5° longitude (11x15) TRANSPAC fields extending from 30°N to 50°N and 160°E to 130°W to the area and gridpoints encompassed by the model (see figure 1).

The first step in preparing the TRANSPAC temperature anomaly data was to interpolate the data from the ten levels of TRANSPAC to 11 intermediate levels of the model, specifically to 0, 20, 45, 80, 125, 200, 325, 600, 1200, 2200 and 4000 meters. Below 400 meters, values were assigned to the intermediate levels by decreasing the 400 meter anomalous temperature to a value of zero at the 2200 meter intermediate level.

This was accomplished by multiplying the 400 meter value by a cosine function which decreased with depth. For example, if T'(400) is the given TRANSPAC anomaly at any grid point, then the anomaly at depth Z, T'(Z), was specified by

$$T'(Z) = T'(400) \cos \left[\left(\frac{Z-400}{1800}\right) \frac{\pi}{2}\right] .$$

This is a very important assumption, since it assumes the temperature anomaly cannot change sign with depth below 400 meters. The resulting temperatures at the 11 intermediate levels were then averaged between any two levels to define the temperature at the ten prognostic levels in the model which are located at 10.0, 32.5, 62.5, 102.5, 162.5, 262.5, 462.5, 900.0, 1700.0 and 3100.0 meters.

The next step in preparing the TRANSPAC data was to expand it to cover the entire area of the model. This was done by expanding the temperature anomaly at the border of the 11x15 TRANSPAC area outward to zero at the outer boundary of the model. In order to provide a smooth transition into the area of no data, the extrapolation was along a sine function as shown in figure 1. Areas of the array which could be filled by both longitudinal and latitudinal extrapolation were assigned a temperature anomaly value which was an average of the two extrapolations. Once the entire geographical area of the model was filled on a 2° latitude by 5° longitude grid, an interpolation scheme was used to fill the 33x33 array of model grid points. The 33x33 array of anomalous temperatures at the ten levels of the model for

September 1976 was then added to the model generated climatology for September 15 to constitute the initial temperature conditions of the model. Similar 33x33x10 arrays for October 1976 to January 1977 served as the verifying data for computing verification statistics for the different model integrations as described below.

III. MODELING APPROACH

In order to test a variety of atmospheric and oceanic processes that may be responsible for the formation and evolution of the large-scale temperature anomalies that are of interest, a series of initial value model integrations have been carried out using a 10-level primitive equation model in a closed rectangular basin. The model is that of Haney (1974) which has been improved to include time dependent seasonal forcing by the atmosphere, a parameterization of surface wind and convective mixing (Haney and Davies, 1976), and nonlinear lateral eddy viscosity based on two-dimensional turbulence theory (Haney and Wright, 1975). The ocean model is driven by wind and differential heating which is calculated from the model sea-surface temperature and prescribed values of the atmospheric solar radiation, total cloudiness, surface air temperature, relative humidity and winds. These quantities are made up of a climatological part and in some cases an anomalous part.

To initialize the model for a prediction experiment, the model is first integrated over a long "spin-up" period (240 years) using climatological atmospheric forcing. The last year of this integration is referred to as the "model climatology" and the resulting currents and temperatures, especially in the mid-ocean areas, bear a close resemblance to those in the North Pacific Ocean. The initial conditions

for the prediction experiments are then obtained by combining a given anomaly, whether oceanic or atmospheric, with the model climatology for the same parameter for the appropriate time of the year.

Once the anomalous atmospheric forcing and temperature anomaly fields were prepared for input into the model, five runs, each with different model configurations, were made. As stated in the introduction, the purpose of the different model experiments was to examine the relative importance of various atmospheric and oceanic processes in the formation and evolution of the observed anomalies.

The five different model integrations are most easily described by writing the equation of horizontal motion and the thermodynamic energy equation as follows, (symbols defined in Table I),

$$\frac{dV_H}{dt} = \frac{1}{\rho_o} \nabla_H p - fK \times V_H + \nabla \cdot (A \nabla V_H) + \frac{\partial}{\partial Z}(K \frac{\partial V_H}{\partial Z}) \qquad (1)$$

$$\frac{dT}{dt} = M(Q, \tau) + \nabla \cdot (A \nabla T) + \frac{\partial}{\partial Z}(K \frac{\partial T}{\partial Z}) \qquad (2)$$

The terms on the right hand side of (1) are the pressure gradient force, the Coriolis force, horizontal momentum diffusion and vertical diffusion. The terms on the right hand side of (2) are the vertical mixing of heat due to the action of surface wind and convection, horizontal diffusion and vertical diffusion. The ocean model is driven by a downward flux of heat and momentum (stress) at the surface which enters through boundary conditions in the vertical diffusion terms:

$$\left(K \frac{\partial T}{\partial Z}\right)_{Z=0} = Q = \text{downward heat flux at the surface}$$

$$\left(K \frac{\partial V_H}{\partial Z}\right)_{Z=0} = \tau = \text{surface stress}$$

In all of the model experiments climatological values of the heat flux, Q, were used. The stress, τ, was calculated from

$$\tau = \rho_a C_D |V_S| \, V_S \, ,$$

where V_S is a prescribed surface wind which is the sum of a climatological part and an anomalous part; the latter being calculated from Namias' sea level pressure anomalies described above. Thus, only V_S has an anomalous part, say V_S' and it enters the model equations in two places; as a boundary condition (wind stress) in the vertical diffusion term, $\left(K \frac{\partial V_H}{\partial Z}\right)_{Z=0}$; and directly in the vertical mixing term $M(Q,\tau)$. The ability exists in the model then to allow the anomalous surface winds to enter into either, both or neither of the terms. In this way, we examine separately the role of anomalous wind driven currents and anomalous wind generated vertical mixing in the generation of oceanic thermal anomalies.

In physical terms, the first model configuration, model 1, describes the free evolution of an initial temperature anomaly since $V_S' = 0$ in this model. In model 2, the effect of the anomalous wind stress in driving anomalous Ekman type flow is added, since $V_S' = 0$ only in the mixing term in this model. According to steady Ekman theory this

flow would be 90° to the right of the anomalous surface winds. Model 3 incorporates the effects of anomalous wind stress in both Ekman type flow and surface wind mixing. This mixing process is expected to produce increased vertical mixing in regions of strong anomalous winds. Model 4 is similar in its dynamics to model 2 but has the initial anomalous temperature fields equal to zero. Likewise, model 5 is similar to model 3 but with the initial anomalous temperatures equal to zero. These last two experiments are designed to evaluate the importance of having good initial conditions when making a prediction.

In order to provide a quantitative comparison between the different models, a variety of statistics were computed for the five model cases at 30-day intervals of time. The statistics calculated included the average absolute prediction error, root mean square error and an S1 score associated with the model generated temperature anomalies. The following definitions indicate exactly what was measured by the statistics. Average absolute error and root mean square error are defined as follows: if in a series of N forecasts (i.e. N different gridpoints), F_i represents the i-th forecast and O_i the corresponding observation, the average absolute error is given by

$$\bar{e} = \frac{\Sigma |F_i - O_i|}{N}$$

and the root mean square error by

$$RMSE = \sqrt{\frac{\Sigma(F_i - O_i)^2}{N}}$$

(Brier and Allen, 1951).

The S1 score is a dimensionless measure of the difference between predicted and observed horizontal gradients and is given by

$$S1 = \frac{\Sigma|e_G|}{\Sigma|e_G|}$$

(Teweles and Wobus, 1954),

where e_G is the error in the forecast temperature anomaly gradient in the horizontal and G_L is the observed temperature anomaly gradient. The S1 score was further divided in order to measure the skill in forecasting both the north-south and the east-west gradient of the temperature anomaly.

The various model predicted and TRANSPAC derived temperature anomaly fields were compared beginning with the October 1976 fields at 30-day intervals of time and at nine levels of the model. Statistics were computed only over an area from 35°N to 45°N and 130°W to 180°. The verification was restricted to the region east of the dateline because the region west of the dateline is generally characterized by numerous mesoscale temperature features (Bernstein and White, 1977). Since the intent of this investigation was in part to study present capabilities in modeling large scale thermal anomalies, it was assumed the model could not effectively predict such mesoscale features.

IV. RESULTS AND CONCLUSIONS

A vast amount of data is made available by this study and as is always the case, interpreting such a volume of data in light of the original intentions of the study is difficult. Describing the actual evolution of the thermal anomalies in the observed and various model cases is perhaps the most logical starting point. A later more detailed treatment of the verification statistics themselves will serve to highlight various aspects of the described results.

Since the effects of anomalous wind stress in producing large scale thermal anomalies is considered paramount, a description of the anomalous atmospheric forcing for September 1976 to January 1977 should precede any description of observed or model evolutions of thermal anomalies. Figure 2 shows the anomalous sea-level pressure fields for these months, contoured at 2 mb intervals with shaded areas indicating negative anomalous pressures. These anomalous pressure fields are shown only over the area of the temperature fields given in figures 3 through 8. The September 1976 mean circulation over the central Pacific was dominated by a trough at 700 mb which had progressed to a position south of the Aleutians. Downstream, the western North American ridge became established as an Arctic ridge (Taubensee, 1976). This mean 700 mb trough in the central Pacific is evidenced at the surface by negative anomalous

pressure. In October 1976, the mean 700 mb trough over the eastern Pacific retrograded somewhat, as did the downstream ridge over western North America (Wagner, 1977a). The negative anomalous pressure pattern at sea level is seen in figure 2 to move westward in October, being replaced to the east by positive anomalous pressure associated with the ridge over western North America. The mean 700 mb trough over the central Pacific remained relatively stationary but intensified significantly (2 standard deviations from the mean) from November 1976 to January 1977 (Dickson, 1977; Taubensee, 1977; Wagner, 1977b). This intensification is manifested in the sea level pressure by an extreme deepening of the negative anomalous pressure fields for November through January.

The observed anomalous temperature data for September 1976, November 1976 and January 1977 at 10, 102, 162 and 262 meters are shown in figure 3. The observed evolution during this winter period in the upper level is characterized by extreme cooling over all but the easternmost edge of the area. In the mid-levels (102 and 162 meters), the September field shows an extremely intense disturbance in the monthly mean temperature anomaly at and just east of the dateline. This disturbance propagates westward out of the area by November. The 102 meter level exhibits a general cooling over the winter months, similar to that in the upper level. At 162 meters there is a general trend towards warming with the axis of temperature anomalies shifting from generally

north-south to east-west. The 262 meter field shows a less intense anomaly structure than the mid-levels for September but exhibits a more intense warming along the east-west axis than had occurred by January at 162 meters.

Figure 4 shows the anomaly evolution predicted by model 1 (climatological winds). The dominant feature in the upper levels is the development of an intense, basically mesoscale feature in the western portion of the area. This development is due to the strong north-south advection of mean temperature by the anomalous geostrophic surface currents induced in the model by the intense disturbance in the western part of the basin at mid-levels. This same type of development occurs in the middle and lower levels so that a similar but less intense structure develops in the vertical. These features tend toward a slow westward propagation during the winter months, indicating partial development and movement as free Rossby waves.

Model 2 introduces anomalous winds, but only in the surface stress term (climatological winds are used in the vertical mixing term). Including this effect produces anomalous Ekman type flow in the upper levels which definitely improves the model predictions by cooling the upper layers (see figure 5). The intense mesoscale features in the west produced by the strong north-south advection of mean temperature described in model 1 are still very apparent in the anomaly structure however. These anomalously cold mesoscale features are intensified and expanded in their horizontal scale in the

upper levels by the superposition of the large scale cooling resulting from the anomalous wind stress. In the middle to lower levels there is a general warming, similar to the observed case, which tends to reduce the intensity of the cold eddies.

Model 3 includes the effects of anomalous winds in both the surface stress term and the vertical wind mixing of heat. This wind mixing process would be expected to produce increased vertical mixing in regions of increased surface winds but as seen in figure 6, the results for model 3 do not vary significantly from model 2. In the ocean model, surface wind mixing depends in part on the net surface heat flux. If the net flux is downward, wind mixing occurs, but if the net surface heat flux is upward as it is in this winter case there is little or no wind mixing. Model 3 results then show only slight differences from model 2 in the uppermost layers.

Model 4 includes anomalous winds only in the surface stress term (like model 2) but the initial temperature anomaly is set to zero in order to evaluate the importance of knowing the initial conditions. In this particular winter case of very strong anomalous wind forcing, the temperature anomalies in the upper levels are predicted slightly better than in models 2 or 3, with general cooling over most of the area as seen in figure 7. Results in middle to lower levels are worse, however, with the 102 m level showing development of small scale warm anomalies near 30-35N where cooling actually occurred and the 262 m level showing cooling to the northeast

where warming is observed. It may be noted at this point that the superposition of the results for model 4 with initial anomalous temperature equal zero and model 1 with no anomalous wind forcing will give almost exactly the results observed in model 2. This is clear evidence that in the model, the effects of external (wind) forcing and the effects of internal dynamical development take place rather independent of one another.

Model 5 is the same in its dynamics as model 3 but again the initial anomalous temperature is set to zero. As previously discussed, models 2 and 3 show little variation and as seen in figure 8, model 5 results vary only slightly from model 4.

The actual verification statistics, of course, provide more concrete evidence to the similarity and differences between the various models in successfully describing the evolution of the large scale temperature anomalies as observed. Table II presents these statistics in the following format: nine levels from 10 meters to 1700 meters depth are considered; the ratio of the root mean square error (RMSE) to the RMSE of climatology (a prediction of zero temperature anomaly everywhere) is given as the first number followed by a similarly non-dimensionalized S1 score for 30 day intervals from October 1976 to January 1977. A ratio of RMSE's and S1's were used as a measure of skill for easy interpretation since a ratio less than one indicates skill over climatology whereas a ratio greater than one indicates less skill than

climatology. The skill of a forecast of persistence is also shown. These ratios for 10, 102, 162, and 262 meters have been plotted as a function of time in figures 9a and 9b for easy reference.

The plot of skill as a function of time at 10 meters seen in figure 9a indicates an extremely rapid loss of skill as early as 30 days, followed by improved skill in the models (2, 3, 4 and 5) having wind forcing. Model 1 with no anomalous wind forcing shows no skill after 30 days but models 2 and 3 clearly demonstrate the benefits of considering such anomalous forcing. Surprisingly, models 4 and 5 with zero initial anomalous temperature conditions show constant improvement with time even over models 2 and 3. This would apparently indicate the greater importance of knowing the anomalous wind forcing than of knowing the initial temperature field exactly, especially in a case as this one where the anomalous winds were very strong.

Perhaps the most conspicuous result is the fact that the model predictions at the surface are better when the initial anomaly is zero (model 4 and 5) than when it is the observed anomaly (model 2 and 3). In the latter case, strong geostrophic flow in the north-south direction is induced at the surface and this flow advects the mean isotherms in the model (cold to the north and warm to the south) to produce a large amplitude disturbance in the western third of the basin which does not exist in the observed pattern. As described earlier, the strong meridional flow is due to the

intense anomaly in the initial temperature field at and below 102 meters. One possible explanation for the model discrepancy is that the model simply does not propagate this developing disturbance westward and out of the domain fast enough. However, an examination of the surface anomaly data west of the dateline shows no large disturbance there to which the predicted disturbance in figure 4 could correspond if the model error was simply one of phase error. A second possibility is that in September there existed a compensating deep temperature anomaly (below 400 meters) whose induced vertical shear nearly cancels that induced by the anomaly observed between 102 and 262 meters. In this case, the model assumption that the initial anomaly decreases slowly to zero at depth, without changing sign (see DATA PROCESSING) is wrong. If this second explanation is true, it implies that in order to predict or understand sea surface temperature anomalies, one must measure the anomaly field all the way down to the bottom of the sea. Unfortunately, it will require many case studies of this type before this question is adequately resolved.

The plot of skill versus time for 102 meters in figure 9a shows a somewhat less rapid loss of skill initially but demonstrates a fairly high amplitude oscillation about 1.0 in the 30 to 120 day period of time. Comparison of the curves for models 4 and 5 and models 1, 2 and 3 indicates a relation between these oscillations and the initial temperature conditions since this alternating behavior is not displayed by models 4 and 5.

Figure 9b shows an extreme and rapid loss of skill (compared to climatology i.e. a forecast of zero anomaly) for persistence and the models at 162 and 262 meters. An oscillation in performance characterizes the 162 meter graph. It is important to note also that while models 4 and 5 have greater skill, they are not as good as climatology. The 262 meter plot does not exhibit this oscillatory characteristic, presumably as a result of less intense anomalous initial temperatures at this depth. It is rather disheartening that the model loses skill so fast at these levels. It is surprising too that persistence is also a very bad forecast at these depths which are generally believed to undergo slow changes.

The S1 scores computed to measure skill in predicting the gradient of large scale thermal anomalies are shown in Table I. Models 4 and 5 consistently demonstrate greater skill than either persistence or the other models in predicting gradients. This indicates of course that the ocean model has little skill in computing gradients since any field more closely resembling a zero field possesses greater skill. If the model S1 scores are broken up into north-south and east-west components, however, there is greater relative skill in predicting north-south gradients than east-west gradients.

The results of this study can be summarized as follows. In the upper levels, the models which include anomalous wind forcing show skill over climatology out to 4 months, i.e. the ratio of RMSE of the model to RMSE of climatology is less

than one. However, knowledge of the initial anomalous temperature conditions degrades the prediction skill. Two possible explanations were offered but a variety of additional case studies are needed to properly resolve this problem. In the lower layers (162 to 262 meters), none of the models show skill over climatology and consideration of neither anomalous wind forcing nor initial anomalous temperatures improves the models predictive capabilities. The rather poor model results at these depths are a serious concern because it is not likely that the addition of anomalous heat fluxes to the model predictions will have much effect at these levels. In the future, it is planned to repeat this type of study for cases in which the anomalous atmospheric forcing was very weak and also to repeat the present study adding anomalous heat fluxes being computed by other NORPAX investigations.

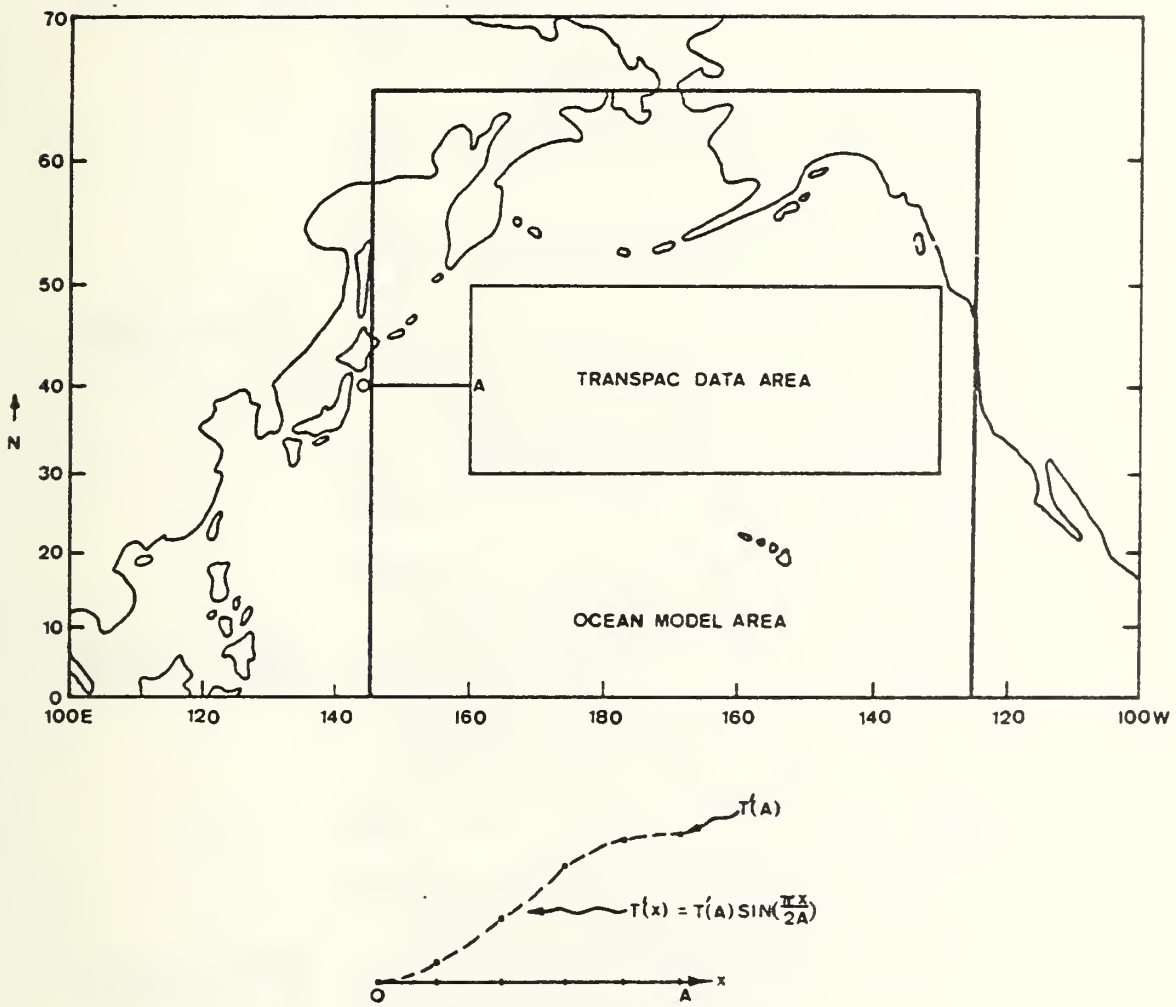
70
60
50
40
30
20
10
0
N
100E
120
140
160
180
160
140
120
100W
A
TRANSPAC DATA AREA
OCEAN MODEL AREA
T'(A)
T'(x) = T'(A) SIN(πx/2A)
O
A
x

Fig. 1

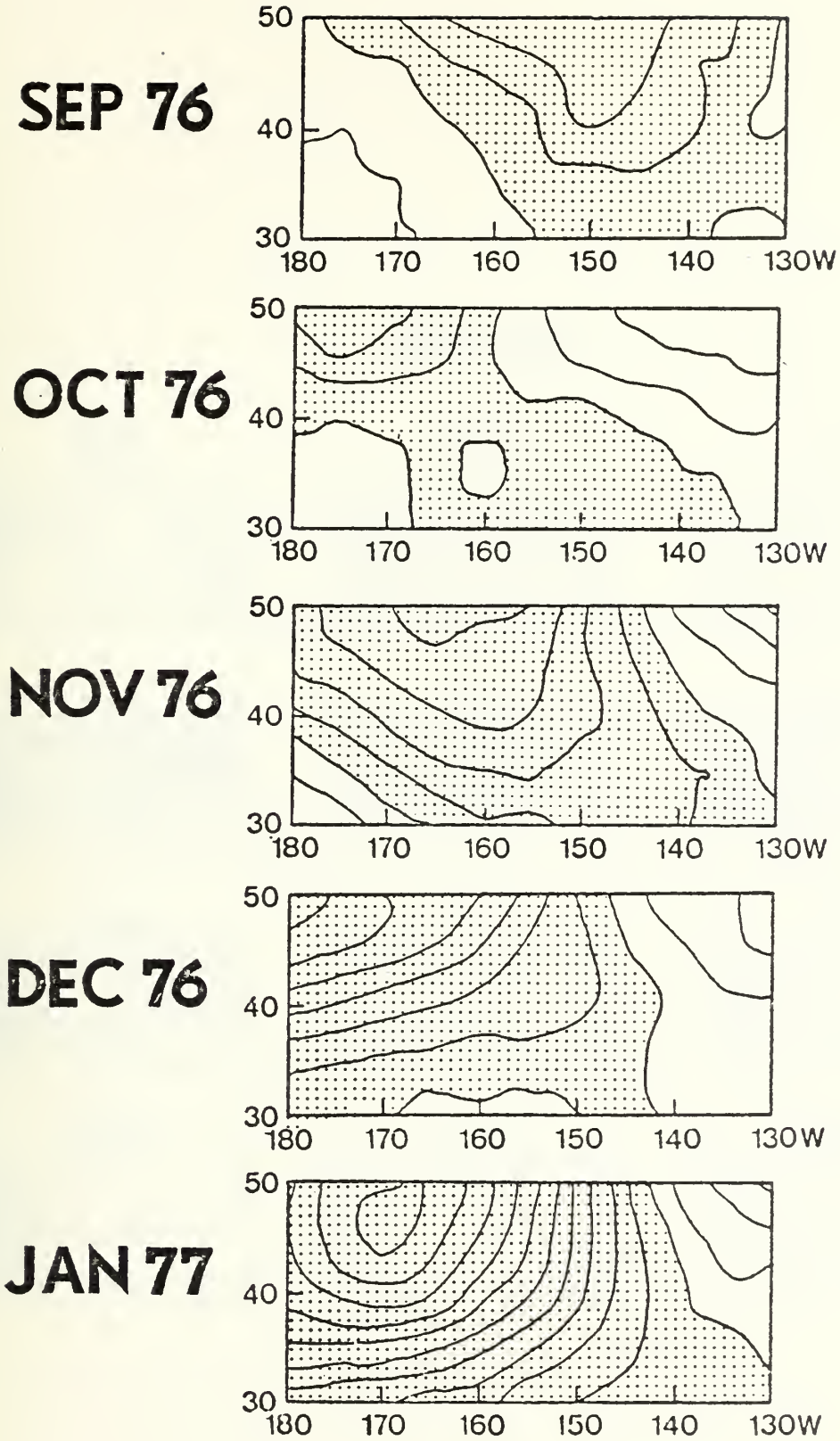
SEP 76
OCT 76
NOV 76
DEC 76
JAN 77
50
40
30
180
170
160
150
140
130W

Fig. 2

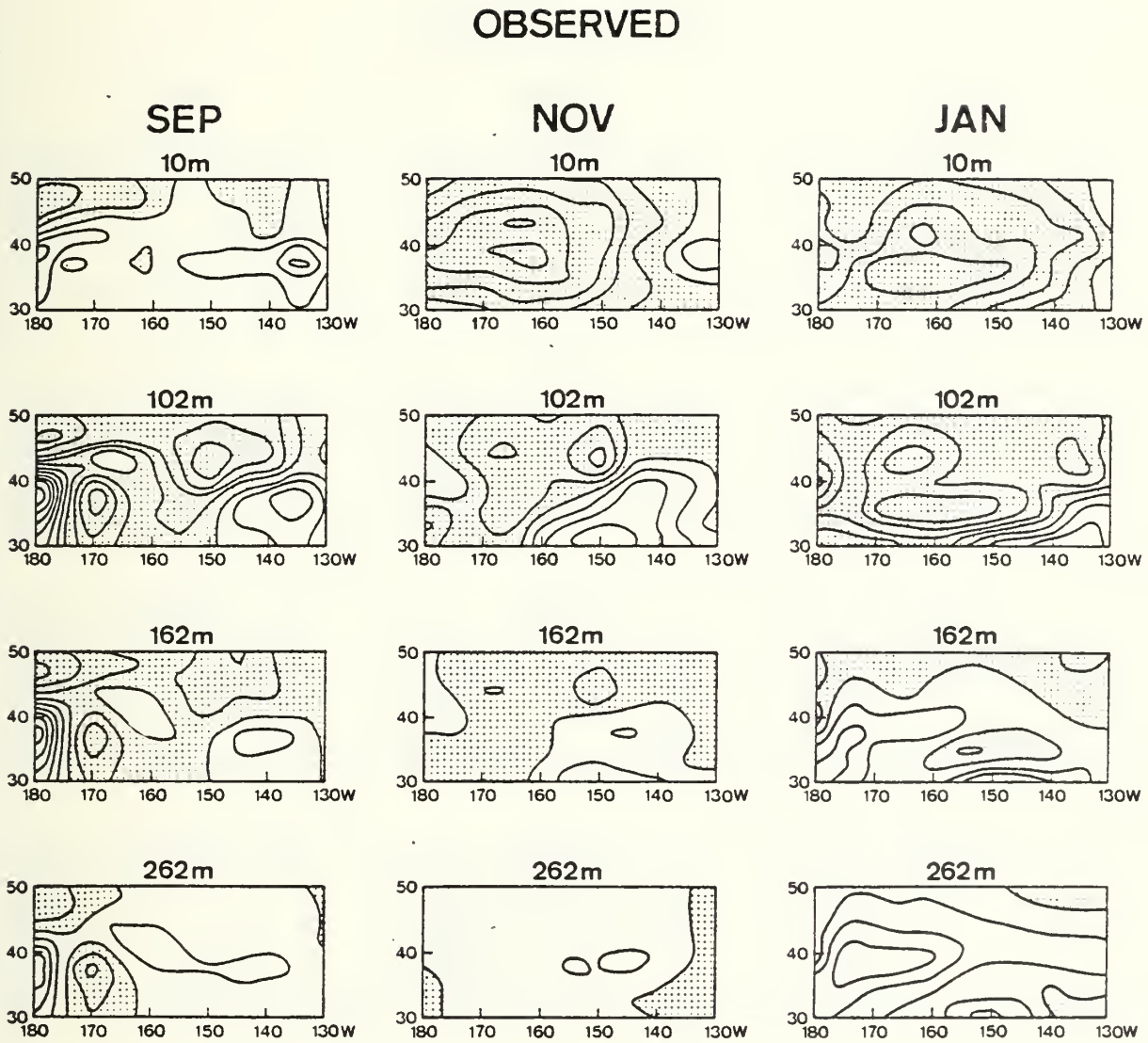
OBSERVED
SEP
NOV
JAN
10m
102m
162m
262m
50
40
30
180
170
160
150
140
130W

Fig. 3

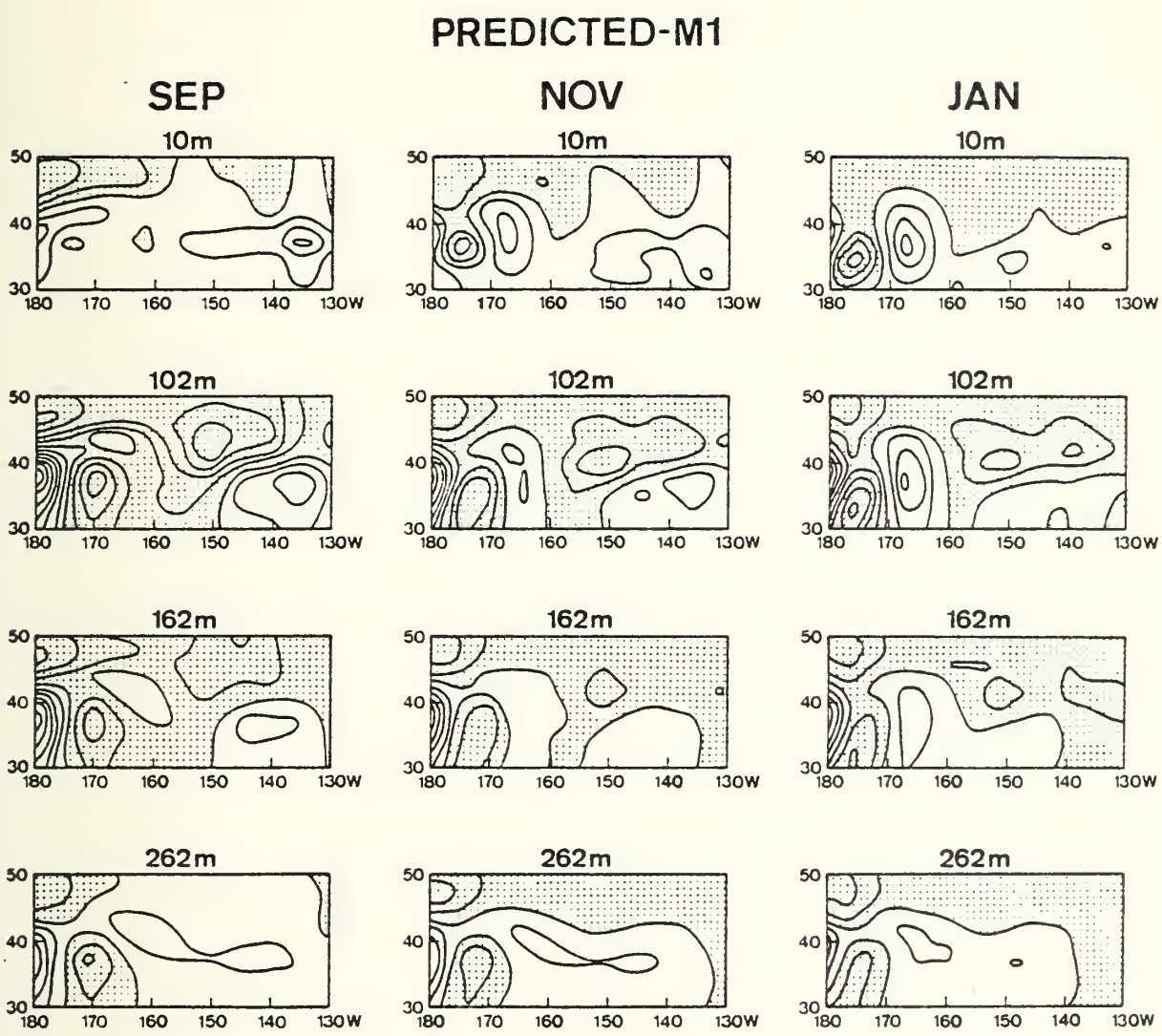
PREDICTED-M1
SEP
NOV
JAN
10m
102m
162m
262m
50
40
30
180
170
160
150
140
130W

Fig. 4

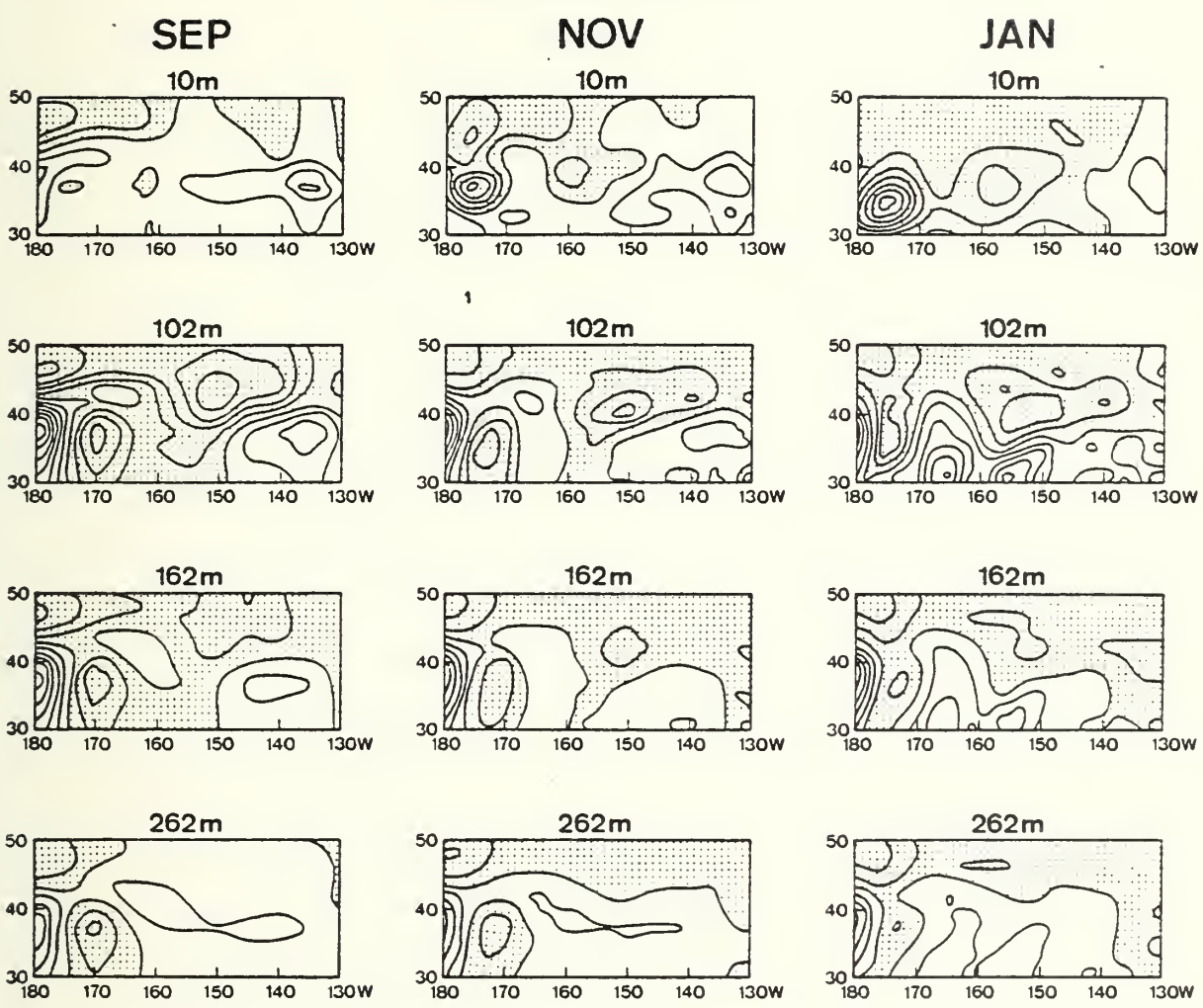
PREDICTED-M2
SEP
NOV
JAN
10m
102m
162m
262m
50
40
30
180
170
160
150
140
130W

Fig. 5

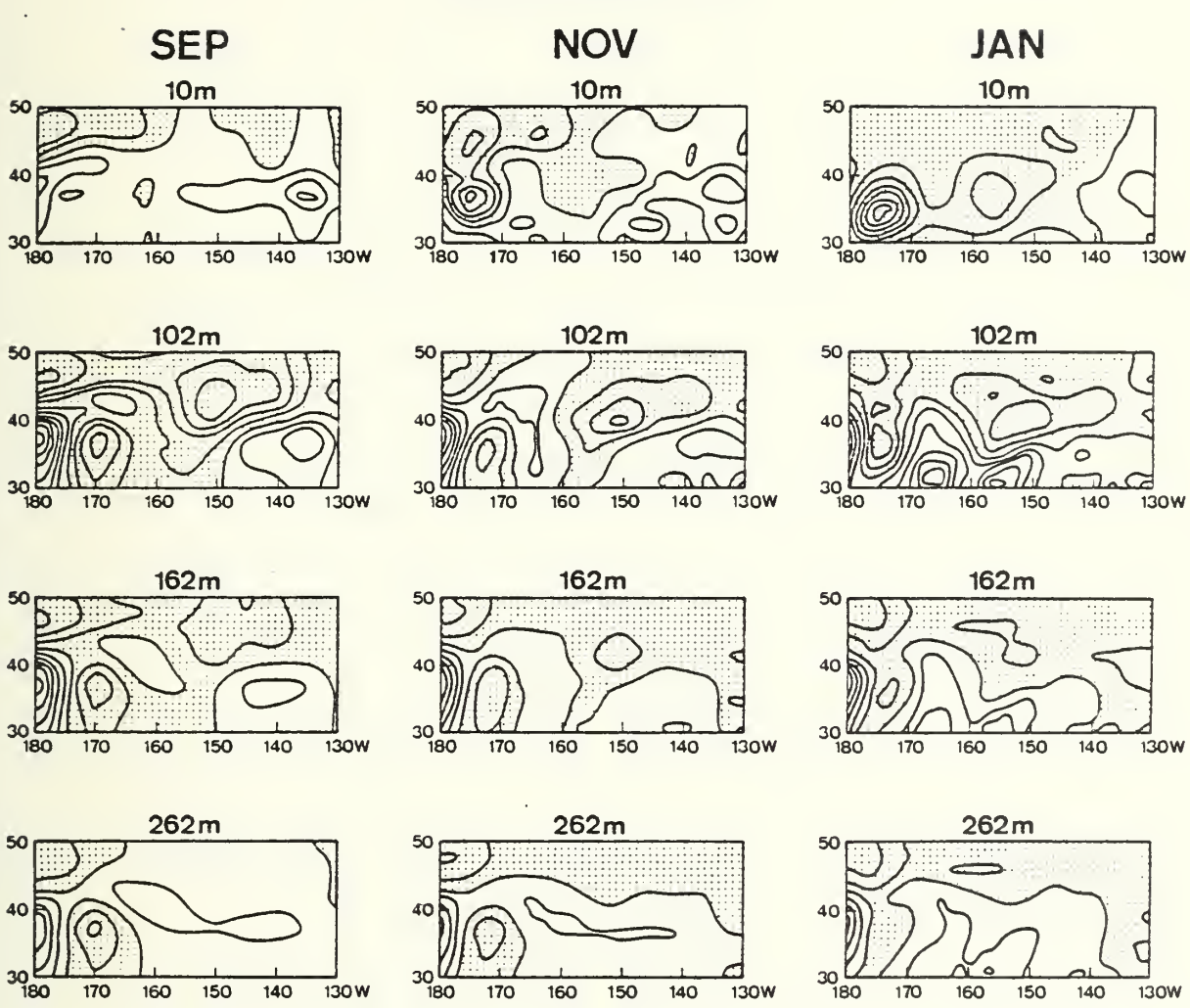
PREDICTED-M3
SEP
NOV
JAN
10m
102m
162m
262m
50
40
30
180
170
160
150
140
130W

Fig. 6

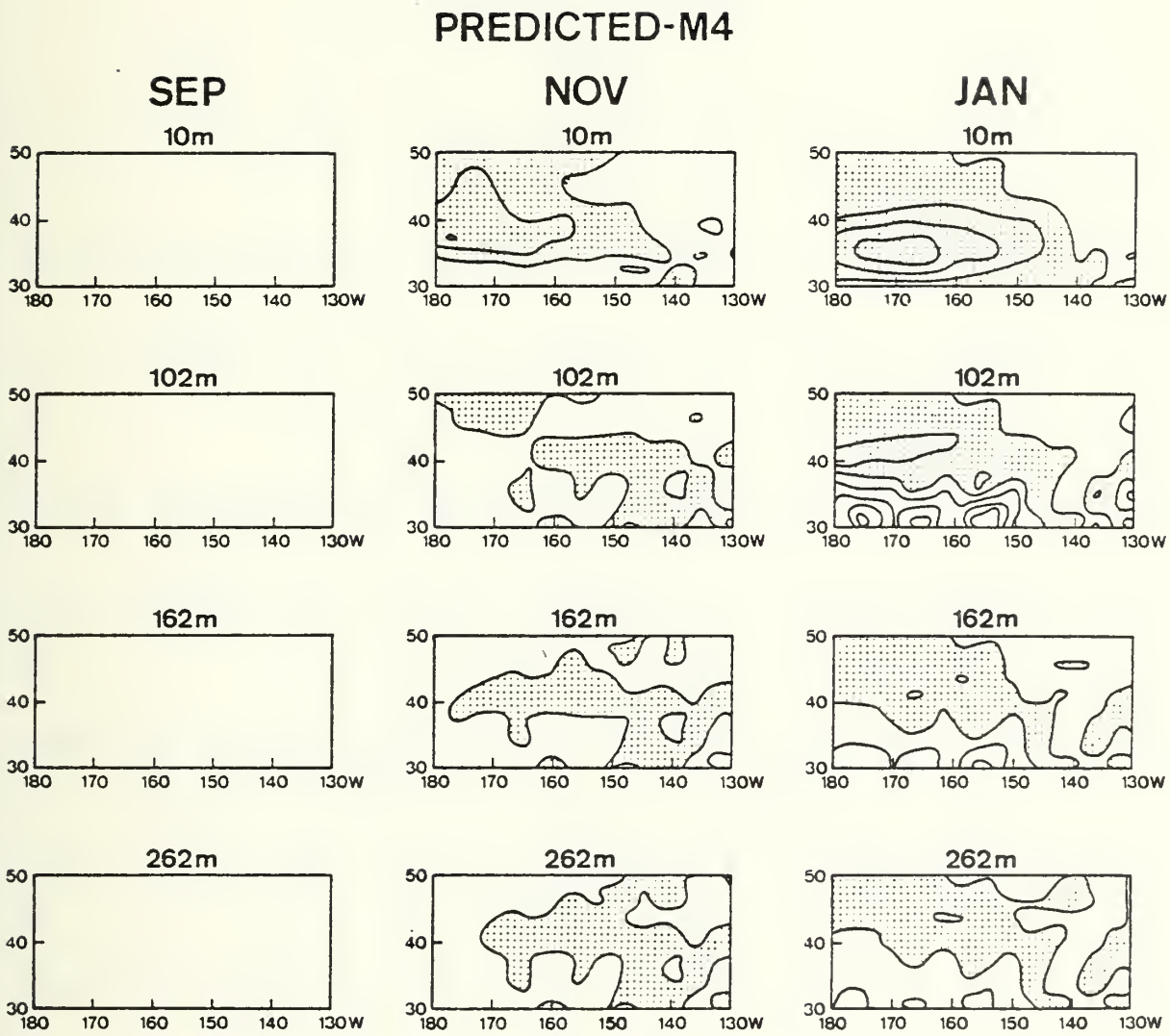
PREDICTED-M4
SEP
NOV
JAN
10m
102m
162m
262m
50
40
30
180
170
160
150
140
130W

Fig. 7

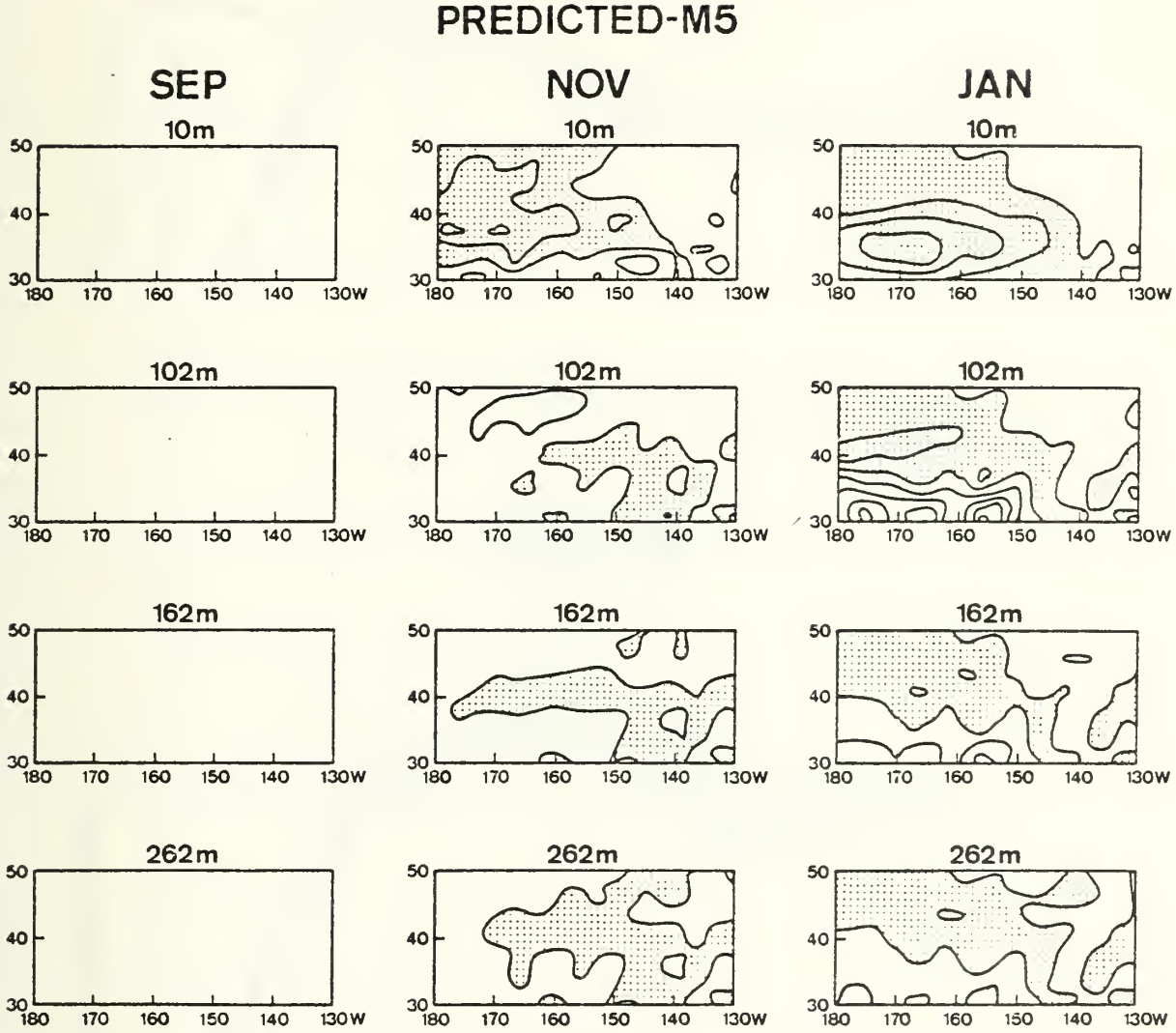
PREDICTED-M5
SEP
NOV
JAN
10m
102m
162m
262m
50
40
30
180
170
160
150
140
130W

Fig. 8

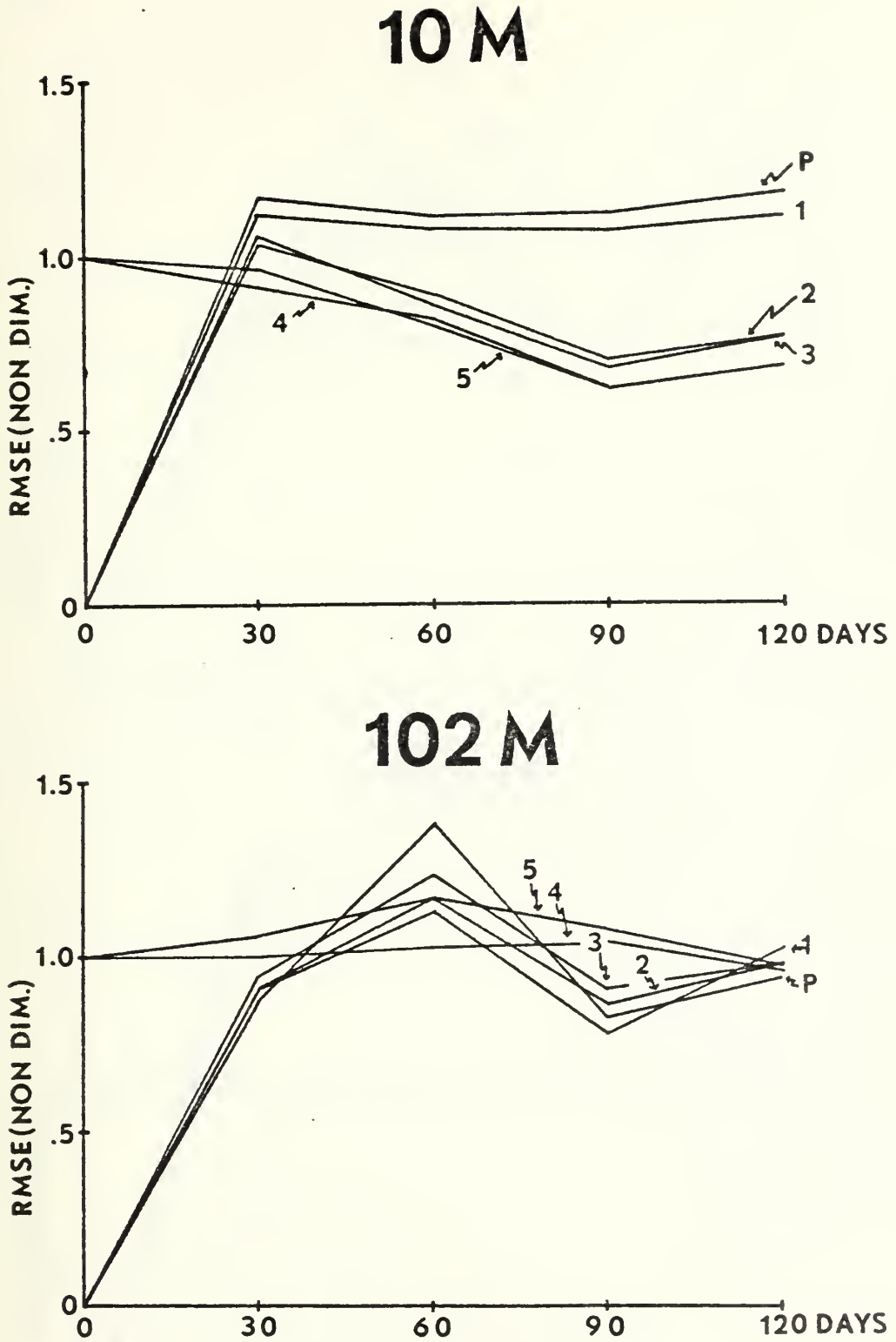
10 M
1.5
1.0
.5
0
RMSE(NON DIM.)
P
1
2
3
4
5
0
30
60
90
120 DAYS
102 M
1.5
1.0
.5
0
RMSE(NON DIM.)
5
4
3
2
1
P
0
30
60
90
120 DAYS

Fig. 9a

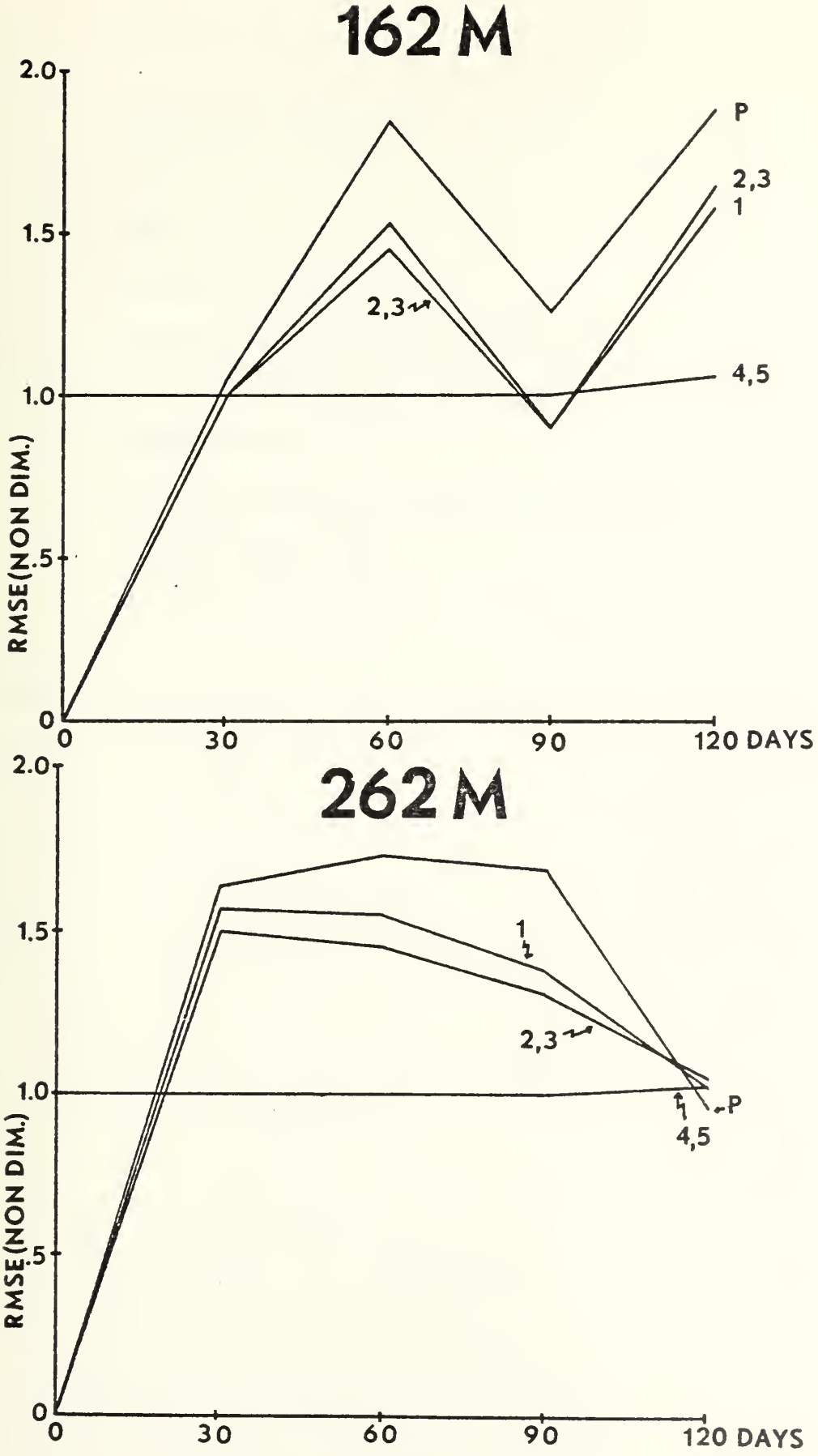
162 M
2.0
1.5
1.0
.5
0
RMSE(NON DIM.)
P
2,3
1
2,3
4,5
0
30
60
90
120 DAYS
262 M
2.0
1.5
1.0
.5
0
RMSE(NON DIM.)
1
2,3
P
4,5
0
30
60
90
120 DAYS

Fig. 9b

V_H = horizontal velocity

ρ_o = reference density

p = pressure

f = Coriolis parameter

A = horizontal diffusion coefficient

K = vertical diffusion coefficient

T = temperature

M = parameterized vertical mixing term

Q = surface heat flux

τ = surface wind stress

TABLE I

10 M (RMSE RATIO/S1 RATIO)				
	OCT	NOV	DEC	JAN
PERS	1.17/1.53	1.11/1.42	1.12/1.61	1.18/1.76
M1	1.12/1.46	1.08/1.61	1.07/1.77	1.11/1.79
M2	1.04/1.48	0.89/1.58	0.70/1.56	0.77/1.52
M3	1.06/1.53	0.87/1.66	0.68/1.57	0.77/1.51
M4	0.92/0.99	0.82/1.05	0.63/0.99	0.69/1.01
M5	0.96/1.13	0.80/1.14	0.62/0.99	0.69/0.99

32 M (RMSE RATIO/S1 RATIO)				
	OCT	NOV	DEC	JAN
PERS	1.18/1.53	1.12/1.50	1.12/1.47	1.13/1.64
M1	1.14/1.48	1.06/1.68	1.07/1.77	1.08/1.85
M2	1.16/1.63	1.01/1.82	0.81/1.56	0.83/1.55
M3	1.08/1.91	0.98/1.90	0.79/1.57	0.83/1.54
M4	1.02/1.08	0.96/1.38	0.75/0.99	0.77/0.95
M5	0.93/1.43	0.93/1.45	0.73/0.98	0.77/0.93

62 M (RMSE RATIO/S1 RATIO)				
	OCT	NOV	DEC	JAN
PERS	1.35/1.23	0.97/1.80	0.94/1.43	0.99/1.83
M1	0.96/1.15	0.99/1.70	0.98/1.56	1.08/1.91
M2	0.99/1.21	1.05/1.94	0.94/1.75	0.81/1.79
M3	1.04/1.36	1.07/2.01	0.95/1.74	0.81/1.79
M4	1.01/0.97	1.05/1.29	0.98/1.36	0.74/1.20
M5	1.06/1.09	1.07/1.41	0.99/1.36	0.74/1.21

Table II

102 M (RMSE RATIO/S1 RATIO)				
	OCT	NOV	DEC	JAN
PERS	0.87/1.22	1.38/1.67	0.84/1.63	0.95/2.29
M1	0.91/1.17	1.14/1.52	0.79/1.32	1.03/1.94
M2	0.91/1.18	1.17/1.55	0.86/1.45	0.98/2.01
M3	0.94/1.24	1.24/1.58	0.91/1.50	0.98/2.02
M4	1.00/0.99	1.03/1.05	1.05/1.21	0.97/1.31
M5	1.06/1.10	1.17/1.14	1.09/1.26	0.98/1.32

162 M (RMSE RATIO/S1 RATIO)				
	OCT	NOV	DEC	JAN
PERS	1.04/1.46	1.85/2.07	1.26/1.80	1.88/1.77
M1	1.00/1.31	1.54/1.91	0.91/1.34	1.59/1.66
M2	1.00/1.32	1.46/1.89	0.91/1.53	1.65/1.74
M3	1.00/1.32	1.46/1.89	0.91/1.53	1.65/1.74
M4	1.00/1.03	1.00/1.10	1.00/1.15	1.06/1.18
M5	1.00/1.03	1.00/1.10	1.00/1.15	1.06/1.18

262 M (RMSE RATIO/S1 RATIO)				
	OCT	NOV	DEC	JAN
PERS	1.64/1.76	1.73/2.29	1.69/2.10	0.97/1.38
M1	1.57/2.03	1.55/2.11	1.38/1.85	1.03/1.38
M2	1.50/2.02	1.45/2.09	1.31/2.00	1.05/1.45
M3	1.50/2.02	1.45/2.09	1.31/2.00	1.05/1.45
M4	1.00/1.02	1.00/1.13	1.00/1.18	1.03/1.11
M5	1.00/1.02	1.00/1.13	1.00/1.18	1.03/1.11

Table II(cont)

462 M (RMSE RATIO/S1 RATIO)				
	OCT	NOV	DEC	JAN
PERS	1.62/1.87	1.00/1.66	1.06/1.81	0.89/1.37
M1	1.62/1.78	0.88/1.35	0.94/1.38	0.86/1.17
M2	1.54/1.77	0.88/1.36	0.89/1.41	0.89/1.24
M3	1.54/1.77	0.88/1.36	0.89/1.41	0.89/1.24
M4	1.00/0.98	1.00/1.03	1.00/1.07	1.06/1.11
M5	1.00/0.98	1.00/1.03	1.00/1.07	1.06/1.11

900 M (RMSE RATIO/S1 RATIO)				
	OCT	NOV	DEC	JAN
PERS	1.45/1.68	0.93/1.44	1.00/1.64	0.86/1.31
M1	1.45/1.58	0.79/1.19	0.93/1.29	0.86/1.11
M2	1.45/1.56	0.79/1.18	0.93/1.30	0.86/1.16
M3	1.45/1.56	0.79/1.18	0.93/1.30	0.86/1.16
M4	1.00/0.99	1.00/1.02	1.00/1.06	1.04/1.08
M5	1.00/0.99	1.00/1.02	1.07/1.06	1.04/1.08

1700 M (RMSE RATIO/S1 RATIO)				
	OCT	NOV	DEC	JAN
PERS	1.50/1.68	0.80/1.44	1.00/1.64	0.82/1.31
M1	1.50/1.58	0.80/1.18	0.83/1.29	0.82/1.11
M2	1.50/1.57	0.80/1.17	0.83/1.30	0.82/1.13
M3	1.50/1.57	0.80/1.17	0.83/1.30	0.82/1.13
M4	1.00/0.99	1.00/0.99	1.00/0.99	1.00/1.02
M5	1.00/0.99	1.00/0.99	1.00/0.99	1.00/1.02

Table II (cont)

LIST OF REFERENCES

Arthur, R. A., "Estimation of Mean Monthly Anomalies of Sea-Surface Temperature," Journal of Geophysical Research, v. 71, p. 2689-2690, 1966.

Bernstein, R. L. and White, W. B., "Zonal Variability in the Distribution of Eddy Energy in the Mid-Latitude North Pacific Ocean," Journal of Physical Oceanography, v. 7, P. 123-126, 1977.

Brier, G. W. and Allen, R. A., "Verification of Weather Forecasts," Compendium of Meteorology, p. 841-848, 1951.

Davis, R. E., "Predictability of Sea Surface Temperature and Sea Level Pressure Anomalies over the North Pacific Ocean," Journal of Physical Oceanography, v. 6, p. 249-266, May 1976.

_____, "A Search for Short Range Climate Predictability," Journal of Physical Oceanography, (in press), 1977.

Dickson, R. R., "Weather and Circulation of November 1976," Monthly Weather Review, v. 105, n. 2, p. 239-244, February 1977.

Haney, R. L., "A Numerical Study of the Response of an Idealized Ocean to Large-Scale Surface Heat and Momentum Flux," Journal of Physical Oceanography, v. 4, n. 2, p. 145-167, April 1974.

_____, and Davies, R. W., "The Role of Surface Mixing in the Seasonal Variation of the Ocean Thermal Structure," Journal of Physical Oceanography, v. 6, n. 4, p. 504-510, July 1976.

_____, and Wright, J., "The Relationship between the Grid Size and the Coefficient of Nonlinear Lateral Eddy Viscosity in Numerical Ocean Circulation Models," Journal of Computational Physics, v. 19, p. 257-266, 1975.

Jacob, W. J., "Numerical Semiprediction of Monthly Mean Sea Surface Temperature," Journal of Geophysical Research, v. 72, p. 1681-1689, 1967.

Kirwan, A. D., Memorandum dated July 9, 1976, Subject: Anomaly Dynamics Study Summary and Five Year Plan, Texas A and M.

Malkus, J. S., "Interchange of Properties between Sea and Air," The Sea, v. 1, Interscience Publishers, p. 88-294, 1962.

Namias, J., "Macroscopic Association between Mean Monthly Sea-Surface Temperature and the Overlying Winds," Journal of Geophysical Research, v. 70, p. 2307-2318, 1965.

Taubensee, R. E., "Weather and Circulation of September 1976," Monthly Weather Review, v. 104, n. 12, p. 1631-1637, December 1976.

_____, "Weather and Circulation of December 1976," Monthly Weather Review, v. 105, n. 3, p. 368-373, March 1977.

Teweles, S. and Wobus, H. B., "Verification of Prognostic Charts," Bulletin of the American Meteorological Society, v. 35, n. 10, p. 455-463, December 1954.

Wagner, A. J., "Weather and Circulation of October 1977," Monthly Weather Review, v. 105, n. 1, p. 553-560, January 1977a.

_____, "Weather and Circulation of January 1976," Monthly Weather Review, v. 105, n. 4, p. 121-127, April 1977b.

INITIAL DISTRIBUTION LIST

		No. Copies
1.	Defense Documentation Center Cameron Station Alexandria, Virginia 22314	2
2.	Library, Code 0142 Naval Postgraduate School Monterey, California 93940	2
3.	Dr. G. J. Haltiner, Code 63Ha Department of Meteorology Naval Postgraduate School Monterey, California 93940	1
4.	Dr. R. L. Haney, Code 63Hy Department of Meteorology Naval Postgraduate School Monterey, California 93940	1
5.	LT. Wayne S. Shiver USN COMPHIBGRU ONE FPO San Francisco 96601	2
6.	Director, Naval Oceanography and Meteorology Building 200 Washington Navy Yard Washington, D. C. 20374	1
7.	Meteorology Department Code 63 Library Naval Postgraduate School Monterey, California 93940	1
8.	LT. K. H. Hunt Fleet Weather Central McAdie Building NAS, Norfolk, Virginia 23502	1
9.	Dr. Joe Huang Great Lakes Environmental Research Lab-NOAA 2300 Washtenaw Avenue Ann Arbor, Michigan 48104	1
10.	Prof. W. L. Gates, Chairman Department of Atmospheric Sciences Oregon State University Corvallis, Oregon 97331	1
11.	Dr. J. Namias Department of Oceanography Scripps Institution of Oceanography La Jolla, California 92093	1

Thesis
S4775
c.1

173205

Shiver
Dynamical numerical prediction of large-scale thermal anomalies in the North Pacific Ocean.